Progress In Electromagnetics Research Letters, Vol. 103, 65–72, 2022

Design of Multiband Band-Pass Filters Based on Novel Associated Band-Stop Resonators

Yi Wu[1, *], Erwan Fourn[2], and Philippe Besnier[2]

Abstract—Although the design of multiband band-pass filters (MBPFs) has been thoroughly studied in the literature, the synthesis of high-order and multiple pass-band filters with controllable transmission zeros (TZs) and high band-to-band isolation is hardly feasible. In this paper, we present a novel design strategy to cope with this issue. Adopting a star-like topology, the proposed design method is based on the parallel association of $N-1$ band-stop stepped-impedance stubs to form an N pass-bands resonator. We show that such a simple design principle allows the accurate control of TZs positions. The principle and theory of these associated band-stop resonators (ABSRs) based filter are exposed, and their efficiency is shown through the synthesis, design, simulation, and measurement of quad-band and quint-band band-pass filters. Very good in-band filter performance and very high band-to-band isolation are achieved for both filters without the need for complex optimization process. These results make the ABSRs an attractive solution to achieve multiple band responses with advanced specifications.

1. INTRODUCTION

Multiband band-pass filters (MBPFs) are essential components in RF systems to achieve multi-standard requirements in communication systems. As a result, many researchers have proposed different synthesis strategies. This includes numerous meaningful works in recent years [1–12]. Various methods and technologies have been proposed to design MBPFs with different levels of complexity, according to the number of bands and order of the filter. However, there are still many challenges when designing MBPFs with more than triple pass-bands and high orders to achieve stringent requirements in a straightforward way.

In the case of quad-band band-pass filters, in [4], a series of second-order MBPFs based on multi-mode stubs loaded ring resonators was proposed. The increased number of loaded stubs enabled to obtain more modes resonating independently. This made reaching more passbands possible. In [5], authors proposed a novel technology to design MBPFs based on a wideband band-pass filter. The transmission zeros (TZs) were introduced by loaded shorted stubs. Therefore, by controlling the number of stubs, MBPFs with multiple passbands can be realized. In [6], a new quad-band band-pass filter is proposed using the properties of asymmetric stepped impedance resonators (SIRs). Two sets of operating passbands working at 2.4/5.2 GHz and the other sets working at 3.5/5.8 GHz were achieved. Some quint-band band-pass filters were also proposed in Reference [7] based on SIRs. There are also other methods to design MBPFs with various topologies and technologies [9–12]. However, it is still difficult to obtain high-order filtering responses and control the positions of TZs independently of each other.

To the best of our knowledge, the synthesis of quad-band or more passband MBPFs with high filter orders, high band-to-band isolation, and flexible TZs is not achieved in the open literature so far. In

Received 11 January 2022, Accepted 15 February 2022, Scheduled 7 March 2022

* Corresponding author: Yi Wu (wuyi51@tju.edu.cn).

[1] School of Microelectronics, Tianjin University, Tianjin 300072, China. [2] University of Rennes, INSA Rennes, CNRS, IETR-UMR 6164, F-35000, Rennes, France.

this letter, we propose an entirely novel star-like topology to design MBPFs over wide frequency ranges in a relative simple way employing associated band-stop resonators (ABSRs). Even though a similar topology was reported in [9] with frequency transformation methods and [10] with a dual-behavior resonator (DBR) topology, the mentioned approaches cannot achieve flexible in-band TZs for the first and high-order filters in an easy way for the second. Moreover, MBPFs based on ABSRs only consist of $N-1$ band-stop resonators to obtain N-bands, leading to more compact structure with respect to these two others. Based on the concept of ABSRs, the proposed MBPFs do not require complex optimization because there are only a few parameters to optimize compared with most of the traditional MBPFs topologies. Also, this method enables fully controllable transmission zeros between each passband and the design of filters, in a relatively easy manner, with a high number of passbands over a wide frequency range, using single layer PCBs. Additionally, the proposed MBPFs exhibit good in-band and out-of-band performance. Another important point is that it is easy to expand them to high-order MBPFs, a challenge for most design methods.

2. PRESENTATION OF THE PROPOSED ABSRS

Figure 1(a) shows the structure of the proposed ABSRs. Each multi-band resonator is composed of $N-1$ short-ended stepped-impedance stubs in a star-like implementation. For simplicity, we assume that the electrical length of each part of a branch i ($i \in [1; N-1]$) of the ABSRs equals $\lambda/4$ (or $\theta_i = \pi/2$) at its resonant frequency f_{zi}, which corresponds to a transmission zero. Calculating the input impedance of each branch and add them together to get the total input impedance of the parallel association of the $N-1$ branches, the total input admittance Y_{tot} can be written as:

$$Y_{tot} = \sum_{i=1}^{N-1} Y_i = j \sum_{i=1}^{N-1} \frac{Z_{i2} \tan^2\left(\frac{f}{f_{zi}}\frac{\pi}{2}\right) - Z_{i1}}{Z_{i1}(Z_{i1}+Z_{i2}) \tan\left(\frac{f}{f_{zi}}\frac{\pi}{2}\right)} \tag{1}$$

where Y_i denotes the input characteristic admittance of the branch i; f is the working frequency; and Z_{i1} and Z_{i2} are the characteristic impedances of the first and the second parts of the i^{th} short-ended stub ($i \in [1; N-1]$), respectively.

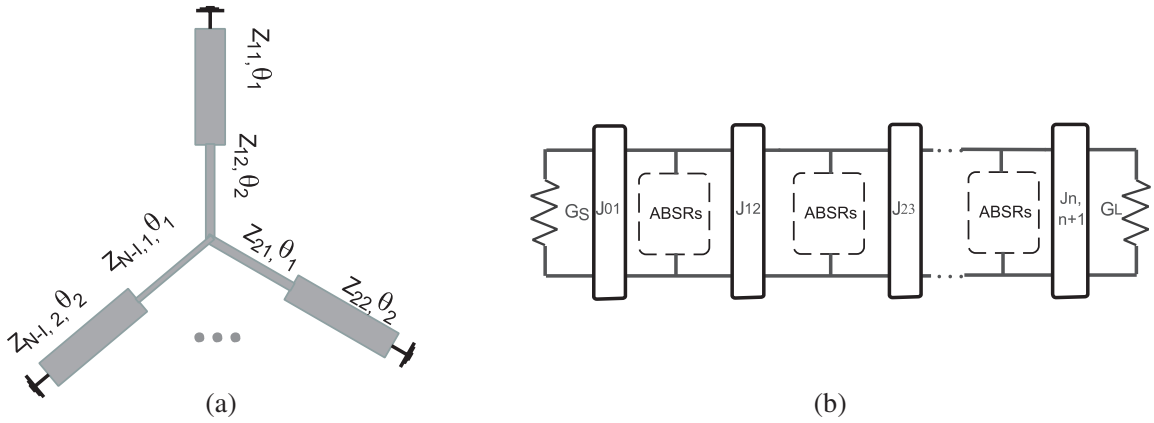

Figure 1. (a) Combined ABSRs on a star topology; (b) topology of MBPFs with associated band-stop resonators.

It is easy to find that the TZs are obtained when $f = f_{zi}$. In this condition, the input admittance goes to infinity, and each TZ frequency f_{zi} determines the length of its associated branch i independently of the others. There are also two additional TZs, the first one at the origin ($f_{z0} = 0\,\text{Hz}$) and the last, called f_{z_N}, which is the first harmonic of f_{z1} ($f_{z_N} = 2f_{z1}$). Of course, these two additional TZs cannot be fixed independently, but they participate in the creation of the first and last bands, respectively. One reflection zero can be obtained between two consecutive TZs leading to a total of N passbands. These

reflection zeros appear when $Y_{tot} = 0$. One should notice that Eq. (1) is nonlinear. As a consequence, the equation bound to the slope parameters is also nonlinear. In order to simplify the filter conception, an optimization is performed to determine the characteristic impedances Z_{i1} and Z_{i2} according to the passband specifications and by considering that the first impedance needs to be as high as possible, and the second one must be relatively low to obtain narrow rejected bands. From the knowledge of the transmission and reflection zeros and the characteristic impedance pairs of each stepped-impedance stub, the slope parameters [1] of each passband can then be determined by :

$$\begin{aligned} b(\omega) &= \frac{\omega}{2} Im\left(\frac{\partial Y_{tot}}{\partial \omega}\right)|_{\omega=\omega_r} \\ &= \frac{\pi}{4}\sum_{i=1}^{N-1}\frac{f}{f_{zi}}\frac{1}{(Z_{i1}+Z_{i2})}\left(\csc^2\left(\frac{\pi}{2}\frac{f}{f_{zi}}\right)+\frac{Z_{i2}}{Z_{i1}}\sec^2\left(\frac{\pi}{2}\frac{f}{f_{zi}}\right)\right). \end{aligned} \tag{2}$$

Figure 1(b) shows a classical ladder-type topology to design the MBPF by associating different ABSRs. The ABSRs are separated with admittance inverters, J_{kl} with $k \in [0, M-1]$ and $l \in [1; M]$, M being the filter order. One interesting point should be pointed out here: as shown in Eq. (2), there are several combinations of impedances and TZs that can achieve the same slope parameters. This allows us to have more freedom degrees to optimize the MBPF. In the two examples presented hereafter, however, we deal only with three identical ABSRs to design third-order multi-band band-pass filters for the sake of simplicity.

3. EXAMPLES OF MULTIBAND BAND-PASS FILTERS

3.1. Quad-Band Band-Pass Filters

A third-order quad-band band-pass filter and its implementation in microstrip technology are proposed in this section as the first example. There are only a few implementation examples for third-order quad-band MBPFs whatever the technology in the literature. By using our proposed ABSRs, there is no specific challenge to design such MBPFs. The arbitrary passband frequencies specifications we have chosen to design this first example are defined as follows:

(i) Pass-Band 1: 1.38 GHz–1.51 GHz (BW: 130 MHz);
(ii) Pass-Band 2: 1.75 GHz–1.85 GHz (BW: 100 MHz);
(iii) Pass-Band 3: 2.10 GHz–2.18 GHz (BW: 80 MHz);
(iv) Pass-Band 4: 2.50 GHz–2.59 GHz (BW: 90 MHz).

To determine the circuit values according to the specified bandwidth, the following steps can be implemented:

(i) Determination of the three TZs, here at 1.60 GHz, 2.00 GHz, and 2.40 GHz. This step fixes the electrical length of each branch of the ABSRs.
(ii) Selection of the impedance pairs of each stepped-impedance stub forming the multiband resonator according to the bandwidth specification. This step is to make sure that all the resonating frequencies are located in the ranges of each individual passband. These frequencies can be determined taking $Y_{tot} = 0$ in Eq. (1). In this example, they are located at 1.410 GHz, 1.800 GHz, 2.155 GHz, and 2.555 GHz. Fig. 2(a) presents the response of a single ABSRs structure obtained with the chosen impedance values (given in the figure legend).
(iii) The admittance inverters' value, J_{01} and J_{12}, are determined using an optimization process considering the passband ripple and each passband bandwidth.

The determination of inverter's values requires optimization process. Nevertheless, the low number of parameters makes this latter simple and fast.

Figure 2(b) shows the theoretical response of the proposed quad-band filter with optimized J values (given in the legend). It is worth pointing out that this type of filters has a quasi-equal ripple characteristic in the pass-bands region. Concretely, the ripple is not perfectly constant in all passbands, but it has little influence on the performance of the filter, and the final response is in accordance with

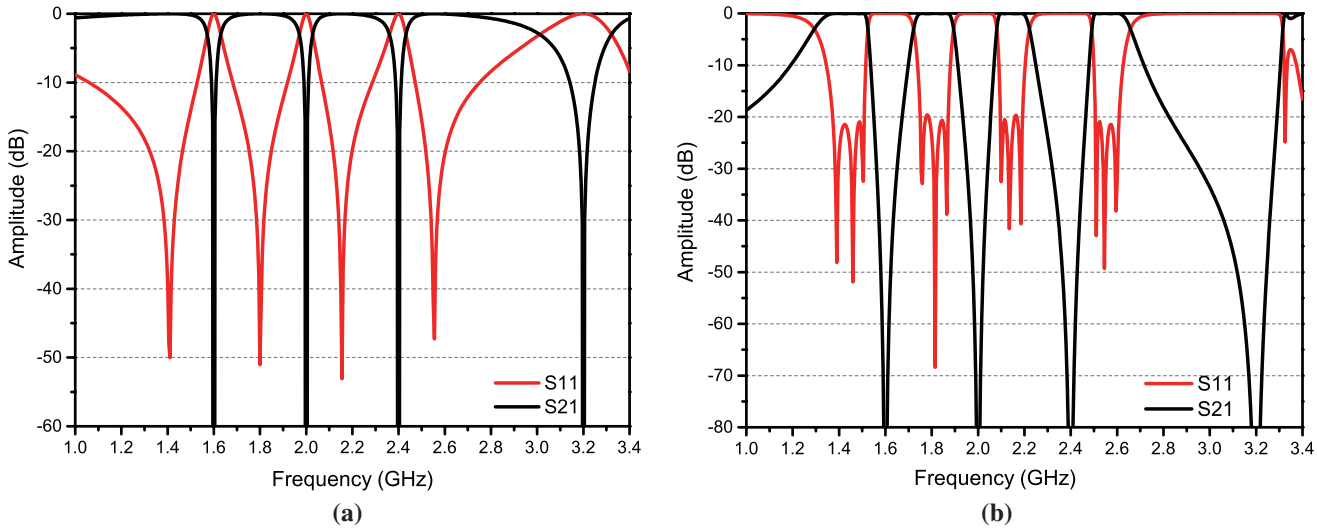

Figure 2. Frequency response of a single quad-band star-like resonator with $Z_{11} = 132.0\,\Omega$, $Z_{12} = 24.0\,\Omega$, $Z_{21} = 138.0\,\Omega$, $Z_{22} = 20.8\,\Omega$, $Z_{31} = 137.9\,\Omega$, $Z_{32} = 24.0\,\Omega$ (a); theoretical responses of the third-order quad-band band-pass filter with $Z_{J01} = 78.0\,\Omega$, $Z_{J12} = 138.5\,\Omega$ (b).

the specifications. For this filter and the following one, the maximum level of the reflection coefficient in passband regions is about 20 dB.

The proposed filter has been implemented in microstrip technology using a RO4003C Rogers substrate (dielectric constant: $\varepsilon_r = 3.55$, height $h = 0.508$ mm, dissipation factor: $\tan\delta = 0.0027$) with copper metallization (metal thickness: $t = 17.5\,\mu$m, conductivity: $\sigma = 5.8 \times 10^7\,\mathrm{S{\cdot}m^{-1}}$). Fig. 3 presents a schematic view of the quad-band band-pass filter with its dimensions. The filter was simulated and optimized using ADS software from Keysight Technologies©, and it was fabricated by laser engraving using an LPKF Protolaser U4. Figure 4 presents a photograph of the fabricated filter, and Fig. 5 presents the EM simulated and measured filter's responses. The fabricated filter's size is $101.5 \times 100.1\,\mathrm{mm}^2$ without taking into account the two $50\,\Omega$ access lines. We can observe good in-band responses and excellent band-to-band isolation of about 60 dB between passbands. The measured return loss for each

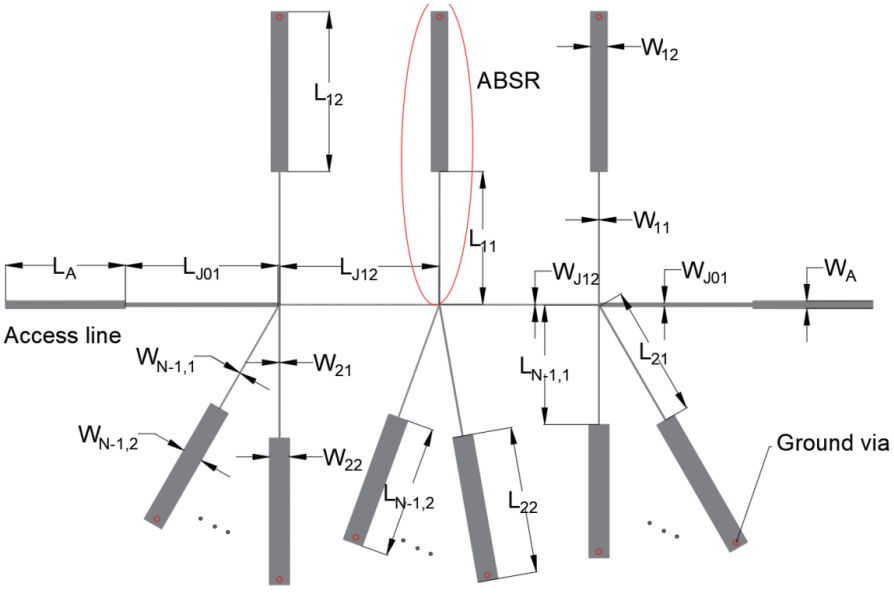

Figure 3. Schematic view of the proposed microstrip N band-pass filter.

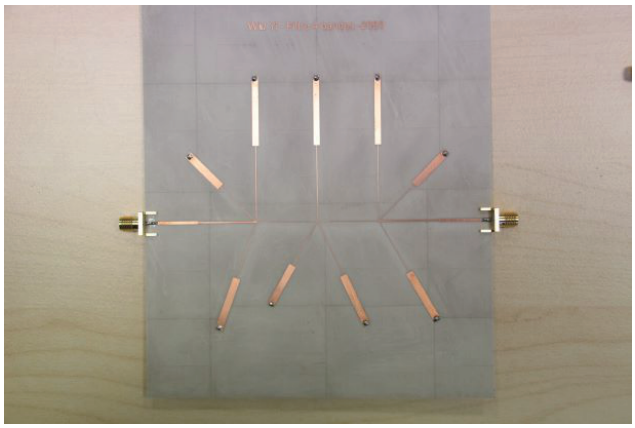

Figure 4. Fabricated circuit of quad-band filter. The dimensions of the filter (all in millimetres) are: $L_{J01} = 23.15$, $W_{J01} = 0.55$, $L_{J02} = 24.00$, $W_{J02} = 0.13$, $L_{11} = 29.90$, $W_{11} = 0.12$, $L_{12} = 27.20$, $W_{12} = 2.50$, $L_{21} = 23.40$, $W_{21} = 0.12$, $L_{22} = 21.50$, $W_{22} = 3.01$, $L_{31} = 19.85$, $W_{31} = 0.15$, $L_{32} = 17.97$, $W_{32} = 3.00$.

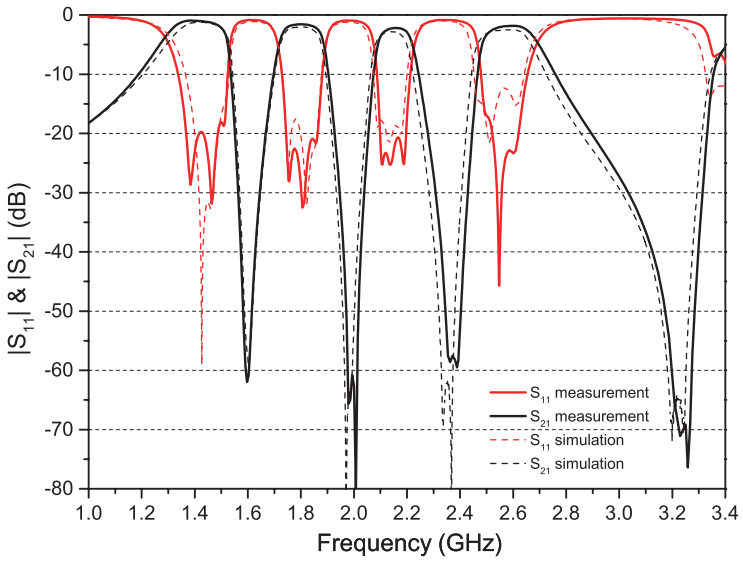

Figure 5. EM-simulated (solid lines) and measured (dotted lines) S parameters of the fabricated quad-band band-pass filter.

band is better than 18.9 dB, 17.6 dB, 17.7 dB, and 12.3 dB, respectively. The measured insertion losses from the first passband to the fourth passband are 1.40 dB, 1.75 dB, 2.53 dB, and 2.10 dB, respectively.

3.2. Quint-Band Band-Pass Filter

Another example of a quint-band band-pass filter based on the proposed ABSRs is presented in this section in order to show the general aspect of the proposed solution. The filter design follows the same steps as for the quad-band band-pass filter presented previously. The arbitrary specifications we have chosen for this second example are:

(i) Pass-Band 1: 1.40 GHz–1.52 GHz (BW: 120 MHz);
(ii) Pass-Band 2: 1.72 GHz–1.82 GHz (BW: 100 MHz);
(iii) Pass-Band 3: 1.98 GHz–2.05 GHz (BW: 70 MHz);

(iv) Pass-Band 4: 2.24 GHz–2.33 GHz (BW: 90 MHz);
(v) Pass-Band 5: 2.56 GHz–2.63 GHz (BW: 70 MHz).

First of all, we choose the four TZs at 1.60 GHz, 1.85 GHz, 2.2 GHz, and 2.5 GHz, respectively. The impedance values of the ABSRs are then chosen following the same procedure and constraints as in the quad-band case. For this second example the impedance values are: $Z_{11} = 140.8\,\Omega$, $Z_{12} = 30.0\,\Omega$, $Z_{21} = 135.0\,\Omega$, $Z_{22} = 22.5\,\Omega$, $Z_{31} = 138.1\,\Omega$, $Z_{32} = 22.4\,\Omega$, $Z_{41} = 140.0\,\Omega$, $Z_{42} = 21.0\,\Omega$. The five resonant frequencies can then be calculated from Eq. (1) with $N = 5$. They are here located at 1.460 GHz, 1.744 GHz, 2.014 GHz, 2.300 GHz, and 2.609 GHz. Fig. 6(b) shows the theoretical response of the proposed quint-band filter with optimized J values (given in the figure's legend). Once again, it is in accordance with the specifications.

This second filter was fabricated under the same conditions as the first. Figure 7 presents a photograph of the fabricated filter, and Fig. 8 presents the EM simulated and measured responses. The

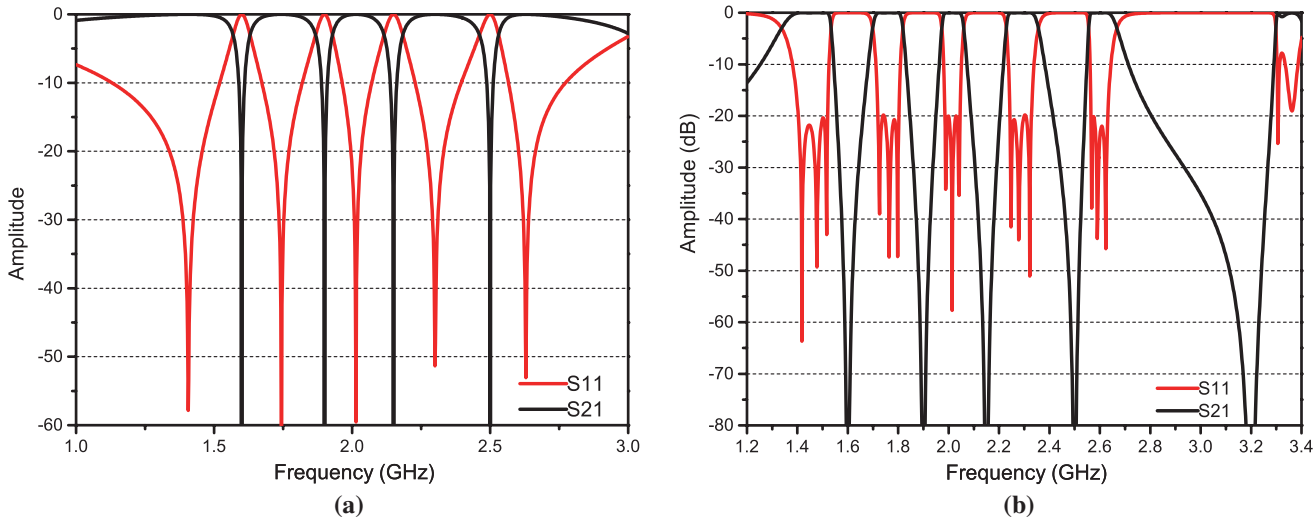

Figure 6. Frequency response of a single quint-band star-like resonator with $Z_{11} = 140.8\,\Omega$, $Z_{12} = 30.0\,\Omega$, $Z_{21} = 135.0\,\Omega$, $Z_{22} = 22.5\,\Omega$, $Z_{31} = 138.1\,\Omega$, $Z_{32} = 22.4\,\Omega$,$Z_{41} = 140.0\,\Omega$, $Z_{42} = 21.0\,\Omega$ (a); theoretical responses of the third-order quad-band band-pass filter with $Z_{J01} = 82.5\,\Omega$, $Z_{J12} = 137.4\,\Omega$ (b).

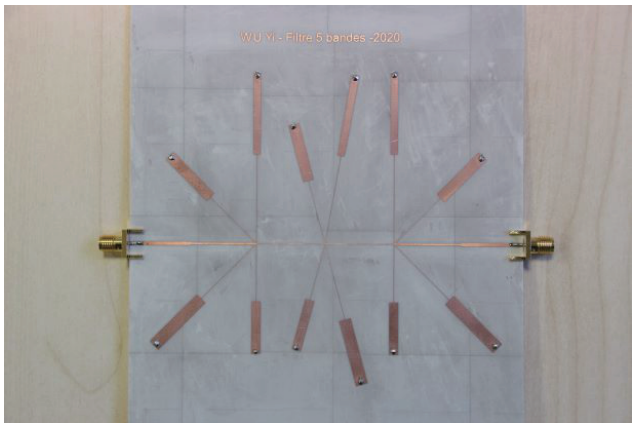

Figure 7. The fabricated circuit for quint-band filter. The dimension of the fabricated filter (all in millimetres) : $L_{J01} = 22.05$, $W_{J01} = 0.53$, $L_{J02} = 22.83$, $W_{J02} = 0.12$, $L_{11} = 29.83$, $W_{11} = 0.12$, $L_{12} = 27.18$, $W_{12} = 2.38$, $L_{21} = 25.90$, $W_{21} = 0.11$, $L_{22} = 22.00$, $W_{22} = 4.02$, $L_{31} = 21.80$, $W_{31} = 0.12$, $L_{32} = 19.40$, $W_{32} = 3.54$. $L_{41} = 19.20$, $W_{41} = 0.10$, $L_{42} = 17.22$, $W_{42} = 3.00$.

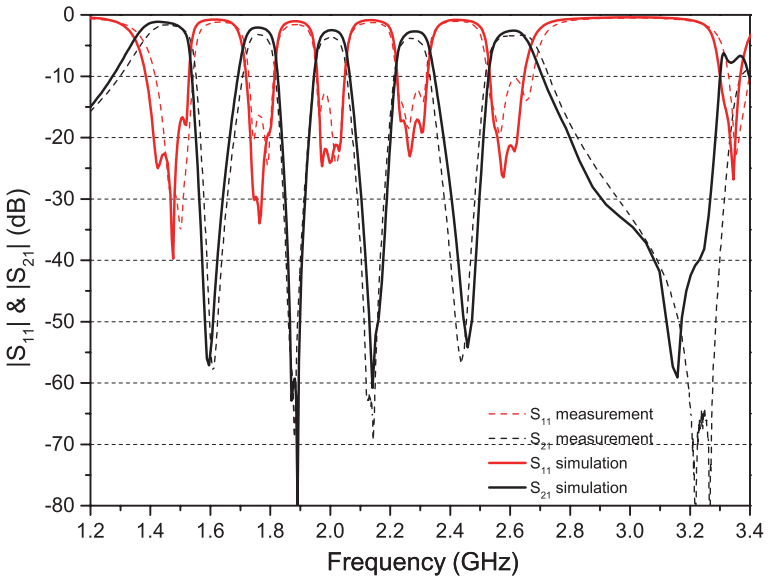

Figure 8. EM-simulated (solid lines) and measured (dotted lines) S-parameters of the quint-band band-pass filter.

fabricated filter's size is $113.4 \times 93.5\,\text{mm}^2$ without taking into account the two $50\,\Omega$ access lines. EM simulations and measurements are in good agreement. Good in-band behaviours and excellent band-to-band isolation better than 50 dB are obtained. The measured return losses from the first band to the last one are better than 20.0 dB, 16.2 dB, 12.9 dB, 12.4 dB, and 10.3 dB, successively. The measured insertion loss for each individual passband is 1.72 dB, 3.22 dB, 3.63 dB, 3.81 dB and 3.37 dB, successively.

4. CONCLUSIONS

In this paper, we propose a simple but powerful synthesis method with ABSRs to design MBPFs. Two examples with four and five bands respectively are studied, simulated, implemented in microstrip technology and measured. Good in-band responses and high band-to-band isolation are easily obtained with a simple procedure. Thanks to the proposed novel star-like topology, we can place a lot of resonators in limited space and achieve high numbers of passbands. All these merits enable us to design high-performance MBPFs simply and quickly.

REFERENCES

1. Hong, J. S. and M. J. Lancaster, *Microstrip Filters for RF/Microwave Applications*, J. Wiley and Sons, New York, USA, 2001.
2. Weng, M.-H., S.-K. Liu, H.-W. Wu, and C.-H. Hung, "A dual-band bandpass filter having wide and narrow bands simultaneously using multilayered stepped impedance resonators," *Progress In Electromagnetics Research Letters*, Vol. 13, 139–147, 2010.
3. Lv, D.-D., L. Meng, and Z. Zou, "Miniaturized HMSIW dual-band filter based on CSRRs and microstrip open-stubs," *Progress In Electromagnetics Research Letters*, Vol. 77, 97–102, 2018.
4. Xu, J., W. Wu, and C. Miao, "Compact microstrip dual-/tri-/quad-band bandpass filter using open stubs loaded shorted stepped-impedance resonator," *IEEE Trans. Microw. Theory Tech.*, Vol. 61, 3187–3199, 2013.
5. Wu, H.-W. and R.-Y. Yang, "A new quad-band bandpass filter using asymmetric stepped impedance resonators," *IEEE Microw. Wireless Compon. Lett.*, Vol. 21, No. 4, 203–205, Apr. 2011.

6. Zhang, Y., L. Gao, and X. Y. Zhang, "Compact quad-band bandpass filter for DCS/WLAN/WiMAX/5G Wi-Fi application," *IEEE Microw. Wireless Compon. Lett.*, Vol. 25, No. 10, 645–647, May 2015.
7. Chen, C., "Design of a compact microstrip quint-band filter based on the tri-mode stub-loaded stepped-impedance resonators," *IEEE Microw. Wireless Compon. Lett.*, Vol. 22, No. 7, 357–359, Jul. 2012.
8. Wu, Y., L. Cui, Z. Zhuang, W. Wang, and Y. Liu, "A simple planar dual-band bandpass filter with multiple transmission poles andzeros," *IEEE Trans. Circuits Syst. II: Exp. Briefs*, Vol. 65, 56–60, 2018.
9. Wu, Y., E. Fourn, P. Besnier, and C. Quendo, "Direct synthesis of multiband bandpass filters with generalized frequency transformation methods," *IEEE Trans. Microw. Theory Tech.*, Vol. 69, 3820-3831.
10. Quendo, C., E. Rius, A. Manchec, et al., "Planar tri-band filter based on dual behavior resonator," *Proc. Eur. Microw. Conf.*, 269–272, Oct. 2005.
11. Garcia, R. G., R. L. Sanchez, D. Psychogiou, and D. Peroulis, "Multi-stub-loaded differentialmode planar multiband bandpass filters," *IEEE Trans. on Circuits and Systems — II: Express Briefs*, Vol. 65, No. 3, 271–275, 2018.
12. Hsu, K. W., J. H. Lin, and W. H. Tu, "Compact sext-band bandpass filter with sharp rejection response," *IEEE Microw. Wireless Compon. Lett.*, Vol. 24, 593–595, 2014.